Involvement of 9-*O*-Acetyl GD3 Ganglioside in *Mycobacterium leprae* Infection of Schwann Cells*□S

Victor Túlio Ribeiro-Resende[‡§1], **Michelle Lopes Ribeiro-Guimarães**[‡], **Robertha Mariana Rodrigues Lemes**[‡], **Ísis Cristina Nascimento**[§], **Lucinéia Alves**[‡], **Rosalia Mendez-Otero**[§], **Maria Cristina Vidal Pessolani**[‡], **and Flávio Alves Lara**[‡]

From the ‡Laboratório de Microbiologia Celular, Pavilhão de Hanseníase, Instituto Oswaldo Cruz, Fundação Oswaldo Cruz, 21045-900 Rio de Janeiro, Brazil and the §Laboratório de Neurobiologia Celular e Molecular, Instituto de Biofísica Carlos Chagas Filho, Centro de Ciências da Saúde, Universidade Federal do Rio de Janeiro, 21941-902 Rio de Janeiro, Brazil

Mycobacterium leprae (ML), the etiologic agent of leprosy, mainly affects the skin and peripheral nerves, leading to demyelization and loss of axonal conductance. Schwann cells (SCs) are the main cell population infected by ML in the nerves, and infection triggers changes in the SC phenotype from a myelinated to a nonmyelinated state. In the present study, we show that expression of 9-*O*-acetyl GD3, a ganglioside involved in cellular anti-apoptotic signaling and nerve regeneration, increases in SCs following infection with ML. Observation by confocal microscopy together with coimmunoprecipitation suggested that this ganglioside participates in ML attachment and internalization by SC. Immunoblockage of 9-*O*-acetyl GD3 *in vitro* significantly reduced adhesion of ML to SC surfaces. Finally, we show that activation of the MAPK (ERK 1/2) pathway and SC proliferation, two known effects of ML on SCs that result in demyelization, are significantly reduced when the 9-*O*-acetyl GD3 ganglioside is immunoblocked. Taken together, these data suggest the involvement of 9-*O*-acetyl GD3 in ML infection on SCs.

Leprosy, one of the oldest recorded diseases, remains an important cause of morbidity, with ~250,000 new cases/year. *Mycobacterium leprae* (ML),[2] the causative agent of leprosy, is an obligate intracellular pathogen with high tropism for Schwann cells (SCs) (1). Data collected over the past 15 years suggest that cell surface molecules are involved in ML adhesion to SCs (2). The G domains of the laminin-α2 chain and the dystroglycan receptor have been shown to play roles in mediating ML attachment to the SC surface (3). Phenolic glycolipid-I, a major unique glycoconjugate on the ML surface, binds laminin-2, which explains the predilection of the bacterium for peripheral nerves (4). *In vitro* and *in vivo* studies in Rag-1$^{-/-}$

mice, which lack B and T lymphocytes, showed that ML attachment to the SC surface is sufficient to cause demyelination in peripheral nerves (5). This effect was found to be dependent on neuregulin receptor, ErbB-2, and ERK 1/2 activation by ML, leading to MAPK signaling and proliferation (6). Additionally, conversion of SCs from the myelinated to nonmyelinated phenotype is directly related to increased proliferative capacity (7). Tapinos *et al.* (8) have shown that ML is able to induce SC proliferation through ERK 1/2 activation via MEK-independent and p56LcK-dependent pathways.

9-*O*-Acetyl GD3 ganglioside is an acetylated glycolipid present in the cell membrane of many types of vertebrate cells (9). This molecule plays an important role in the development, differentiation, and regeneration of the nervous system. Among its multiple functions are: cell attachment to the extracellular matrix, neuronal migration, neurite outgrowth *in vitro*, and control of apoptosis (10–17). 9-*O*-Acetyl GD3 ganglioside is highly expressed after sciatic nerve crush in the regenerating nerve, as well as in the dorsal root ganglia and lumbar spinal cord. During peripheral nerve regeneration, 9-*O*-acetyl GD3 is mainly expressed by SCs, which concurrently undergo changes in phenotype and proliferative state, followed by lower expression in a few axons (18).

The up-regulation of 9-*O*-acetyl GD3 expression in proliferating SCs led us to test the hypothesis that this molecule also plays a role in SC leprosy cytopathology, because proliferative and anti-apoptotic states are also induced by ML during infection (19, 20). We analyzed ML-induced expression of this ganglioside and performed immunoblockage assays in SCs exposed to ML. Moreover, we investigated the association between 9-*O*-acetyl GD3 and well known ML cell ligands (laminin-2, dystroglycan, and ErbB-2 receptors) using laser scanning microscopy and coimmunoprecipitation. These data demonstrate for the first time the involvement of 9-*O*-acetyl GD3 in cellular infection, suggesting a relevant biological role for this ganglioside as a possible receptor for ML in SCs.

EXPERIMENTAL PROCEDURES

Mycobacteria—Armadillo-derived lethally irradiated *M. leprae* was kindly provided by Dr. Patrick J. Brennan (Colorado State University, Fort Collins, CO, through the NIAID, National Institutes of Health under contract 1Al 25469). *M. leprae* (viable and lethally irradiated) derived from the footpads of athymic nu/nu mice were provided by J. L. Krahenbuhl

2 The abbreviations used are: ML, *M. leprae*; FITC+, *M. leprae* conjugated with fluorescein; SC, Schwann cell; MOI, multiplicities of infection; HLP, histone-like protein; HPTLC, high performance thin layer chromatography; ANOVA, analysis of variance; MBP, myelin basic protein; LAM, lipoarabinomannan.

(National Hansen's Disease Programs Laboratory, Baton Rouge, LA). *Mycobacterium smegmatis* mc^2 155 and *Mycobacterium bovis* BCG Pasteur strains were grown at 37 °C in Middlebrook 7H9 broth (BD) supplemented with 0.05% Tween 80 under constant agitation on a magnetic plate. The cultures were harvested in the mid-log phase, counted according to protocol of Shepard and McRae (21), and kept frozen at −70 °C until use. Mycobacteria were conjugated with fluorescein (FITC$^+$; Sigma) by incubation with carbonate-bicarbonate buffer, pH 8.2, for 1 h followed by three washes with 10 mM PBS, pH 7.4.

Culture Procedures—Human SCs derived from the tumor cell line ST-8814 were seeded on coverslips pretreated with poly-L-lysine (100 μg/ml; Sigma-Aldrich) and laminin (10 μg/ml; Invitrogen) in 24-well cell culture plates (Greiner Bio-one). The cultures were then incubated at 37 °C, 5% CO$_2$ in RPMI 1640 medium (Invitrogen) plus 10% FBS (Cutilab, São Paulo, Brazil), penicillin, and streptomycin (100 units/ml and 100 μg/ml, respectively; Sigma). Forty-eight hours later, FITC$^+$ *M. leprae* were added to the culture medium at various multiplicities of infection (MOI, 1:10, 1:25, and 1:50). The cultures were then incubated for 2, 12, 24, 48, and 72 h, followed by gentle removal of the medium. The cells were then washed twice for 2 min with 10 mM PBS, fixed for 15 min with 4% paraformaldehyde (Sigma-Aldrich) at 37 °C, and washed twice again with 10 mM PBS, pH 7.4.

Mouse Infection with M. leprae—Two-month-old male Fox$^{nu/nu}$ (NUDE) mice derived from the Balb-C strain were housed at the Fundação Oswaldo Cruz rodent facility under internal license number P-0328/07. All of the experiments were performed following the National Institutes of Health Guidelines for the Care and Use of Laboratory Animals and were approved by Fundação Oswaldo Cruz Committee for the Use of Experimental Animals. One injection of 10 μl of RPMI medium containing ~10^7/ml live bacteria was administered to each forepaw. Four months after the injection, we were able to observe swelling, indicating that the infection was well established in the injected mice. Ten months after infection, the mice were sacrificed in a CO$_2$ chamber. The sciatic nerves ($n = 4$) were carefully removed and fixed in 4% paraformaldehyde overnight. Sciatic nerves from noninfected NUDE ($n = 4$) and Balb-C ($n = 3$) mice were also removed and fixed for later analysis as control groups. After fixation, all of the nerve segments were cryoprotected with 30% sucrose in 0.1 M phosphate buffer, pH 7.4, for 48 h.

Immunofluorescence—Dissected nerves were embedded in Tissue-Tek® O.C.T. compound (Sakura Finetechnical, Tokyo, Japan). Frozen longitudinal sections were cut at 16 μm on a cryostat (Leica CM 1850), mounted on gelatin-coated slides, and frozen. For immunofluorescence, the nerve sections were washed three times with 10 mM PBS, pH 7.4, and then blocked by incubation with 10% normal goat serum (Invitrogen) and 1% BSA (Sigma) for 1 h at room temperature. Incubation with the primary antibodies was performed overnight at 4 °C, followed by three washes with 0.001% Triton X-100 (5 min each) and then incubation with the secondary antibodies for 2 h at room temperature. The following primary antibodies were used in double or triple labeling combinations for nerve staining in the

in vivo studies: polyclonal IgG anti-α-S100 (1:400; Dako), monoclonal IgM anti-α-9-*O*-acetyl GD3 (Jones clone, 1:100; Sigma), polyclonal IgG anti-α-myelin basic protein (MBP, 1:200; Abcam), and mouse monoclonal IgG anti-α-histone-like protein (HLP, 1:600) or rabbit polyclonal IgG anti-α-Lam (1:35, both kindly donated by Dr. Patrick Brennan).

For immunostaining of SC cultures, fixed cells were washed three times with 10 mM PBS, pH 7.4, and blocked by incubation with 5% normal goat serum (blocking solution) for 40 min in a humid chamber. Primary antibodies were diluted in the blocking solution, and coverslips were incubated for 2 h in a humid chamber at room temperature. Next, the coverslips were washed with 10 mM PBS, pH 7.4 (three times for 5 min each) and incubated with secondary antibodies diluted in the same blockage solution for 90 min at room temperature. After a final series of washes in PBS (three times for 5 min each), the cell nuclei were counterstained with DAPI (Sigma-Aldrich), and each coverslip was placed upside down on a slide containing a drop of SlowFade® antifade solution (Molecular Probes). The following antibodies were used for immunostaining: rabbit polyclonal anti-α-S100 (1:400; Dako), goat polyclonal anti-α-laminin-2 (1:100; Santa Cruz Laboratories), rabbit polyclonal IgG anti-α-laminin (1:1000; Sigma), rabbit polyclonal IgG anti-α-ErbB-2 (1:150; Abcam), mouse monoclonal IgM anti-α-9-*O*-acetyl GD3 (Jones, 1:100; Sigma), mouse monoclonal IgG anti-β-dystroglycan (1:100; Abcam), and mouse monoclonal IgG anti-α-HLP (histone-like protein, 1:600, kindly donated by Dr. Patrick Brennan). The following secondary antibodies were employed: Cy3-conjugated α-mouse (1:800; Jackson Immunochemicals), Cy3-conjugated α-μ chain IgM (1:600; Jackson Immunochemicals), Alexa 488-conjugated α-rabbit (1:400; Invitrogen), Alexa 633 α-mouse (1:400; Invitrogen), Alexa 555 α-rabbit (1:400; Invitrogen), and fluorescein-conjugated rabbit α-goat (1:100; Sigma-Aldrich).

Immunoblockage and Deacetylation of 9-O-Acetyl GD3—ST-8814 SCs (5×10^4/coverslip) were allowed to grow for 48 h in standard medium (RPMI 1640 plus 10% FBS) until semi-confluent. For immunoblockage assay, the cells were incubated in four different conditions: 1) RPMI medium plus 10% FBS as a control condition; 2) Jones antibody added to the standard medium diluted 1:100, as described by Santiago *et al.* (22); 3) mouse IgM immunoglobulin (1:200; Caltag, Burlingame, CA) added to the standard medium as an antibody control; and 4) anti-A2B5 antibody against gangliosides derived from the C-series of the biosynthetic pathway (1:50; Roche Applied Science). For the deacetylation assay, cultured Schwann cells were incubated for 1 h at 4 °C in the absence of light in three different conditions: 1) RPMI medium plus 10% FBS as a control condition; 2) 10 mM of meta sodium periodate (NaIO$_4$) (Sigma), as described by Van Lenten and Ashwell (23) and Manzi *et al.* (24); and 3) Jones antibody added to the standard medium diluted 1:100 in control medium. The cells were incubated for 2 h with the Jones antibody before bacteria addition to the cultures. The medium containing NaIO$_4$ was removed, and cells were washed twice in 10 mM PBS, pH 7.4, and incubated with control medium. Two hours after incubation in both experimental conditions, FITC$^+$ *M. leprae* (MOI 1:25) were added to the cultures and incubated for additional 24 h. The SCs were then washed

and fixed, immunolabeled for S100, and mounted as described above. Two independent experiments were performed in a total of six wells ($n = 6$) for each experimental condition.

For proliferation assays, SCs were incubated for 48 h after immunoblockage, followed by fixation and immunostaining for Ki-67 (1:150; Abcam), and the cell nuclei were counterstained with DAPI. Neutralizing antibody to GD3 ganglioside, the direct precursor of 9-*O*-acetyl GD3, was added to the SC culture as a ganglioside blockage control group, as was GD2 ganglioside, which belongs to the b-series of ganglioside biosynthesis. Two independent experiments, each with six replicates, were performed for each experimental condition.

Blockage of β-1 Integrin Receptor—Human Schwann cells (ST-8814) were cultured until semi-confluence in RPMI medium supplemented with 10% FBS. Then 50 ng/ml of β-integrin blocking peptide (Santa Cruz Laboratories) was added to the medium. The cells were incubated for 2 h before immnunoblockage procedure with mAb Jones, and controls (RPMI, mouse IgM, and A2B5) were repeated as described previously. Again, 2 h after immunoblockage, FITC$^+$ *M. leprae* (MOI 1:25) were added to the cultures. Both blocking peptide and mAb Jones were kept for 24 h during incubation with bacteria.

Microscopy Image Capture and Analysis—Slides containing immunolabeled SCs were analyzed by epifluorescence microscopy (Apotome; Zeiss) using rhodamine, fluorescein, and DAPI filters. The images were captured by digital camera (Axiocam; Zeiss) coupled to imaging software (Axiovision; Zeiss). Optical sections, images for colocalization analysis, and tri-dimensional reconstruction for both *in vivo* and *in vitro* experiments were obtained by confocal microscopy (LSM 510 Meta; Zeiss) using lasers with 488-, 583-, and 633-nm wavelengths.

Ganglioside Extraction and Identification by High Performance Thin Layer Chromatography (HPTLC)—The total lipids of cells were extracted from 1 mg of total protein for each experimental condition with 10 volumes of chloroform/methanol (1:1 v/v; Merck) and separated into two equal samples. One sample was treated with a mild alkaline solution of 2 N NaOH at 37 °C for 1 h and neutralized with a solution of 2 N acetic acid. This sample was called base-treated. Both samples were then separated using a Lipophilic Sephadex LH-20 column chromatograph, and only the ganglioside fraction was recovered. Individual gangliosides were separated by HPTLC using plates of silica gel 60 (Merck). GM1 and GM2 gangliosides were used as standards. The separation was performed with chloroform/methanol 1:1 (v/v) for 10 min, followed by chloroform/methanol/CaCl$_2$ (50:45:10 v/v/v) for 45 min. To detect glycolipids in the sample, the plates were stained with a solution of 5% H$_2$SO$_4$ and 0.1% orcinol and baked at 120 °C for ~3 min. For immunological overlay assays, the HPTLC plate was treated with 0.4% polyisobutylmethacrylate in hexane/chloroform. Nonspecific binding sites were blocked with 1% BSA in PBS for 45 min. The plate was then incubated with Jones mAb (1:200) in 10% fetal calf serum overnight at 4 °C and washed five times with 10 mM PBS at pH 7.4, followed by incubation with an anti-IgM HRP-conjugated antibody (1:400; Sigma) in 10% FCS for 2 h at room temperature and five further washes with PBS. The immunoreactive bands were observed using an enhanced chemiluminescence ECL kit (Amersham Biosciences).

Coimmunoprecipitation and Western Blotting—After incubation, SCs were washed twice with 10 mM PBS at pH 7.4 plus 0.2 mM sodium orthovanadate and 1 mM PMSF (Sigma) at room temperature. Radioimmune precipitation assay buffer was added to the plates to lyse cells, and the mixture was incubated for 20 min at 4 °C, followed by DNA shearing. The lysate was transferred to a small tube and centrifuged for 15 min at 2500 × *g*. The supernatant was then centrifuged again at 13,000 × *g* for 20 min. The protein content of supernatants was assayed by a BCA kit (Pierce). Jones IgM mAb (1:100) was added to equal amounts of protein (1 mg), and the lysates were incubated at 4 °C for 2 h with light shaking. Next, 50 μl of protein L-agarose was added and incubated at 4 °C for 1 h. The immunocomplexes were recovered by centrifugation at 1000 × *g* at 4 °C for 1 min and washed twice with radioimmune precipitation assay buffer plus 1 mM PMSF, once with TBS, twice with 0.5 M Tris, pH 6.8, and stored at −70 °C.

For Western blotting, the immunocomplexes were treated with sample buffer and resolved by SDS-PAGE on 8.5 or 6% gels, followed by transfer to nitrocellulose membranes. After blocking with TBS plus 3% BSA for 2 h at room temperature, the membranes were incubated with anti-laminin-2 (1:200, goat polyclonal; Santa Cruz Biotechnology), anti-β-dystroglycan (1:100, rabbit polyclonal; Abcam), or anti-ErbB-2 (1:200, rabbit polyclonal; Abcam,) for 2 h at room temperature. Protein bands were visualized by incubation with mouse anti-goat or goat anti-rabbit horseradish peroxidase-conjugated antibody (1:400; Sigma) and chemiluminescent Supersignal substrate (Pierce).

Quantitative and Statistical Analysis—Data were analyzed using one-way analysis of variance (ANOVA) with Neuman-Keuls post-test for multiple comparisons. The results are expressed as the means ± S.E.

For quantification of 9-*O*-acetyl GD3 expression in SCs infected with ML, five photomicrographs were taken per coverslip, and the percentage of 9-*O*-acetyl GD3 positive SCs was calculated compared with the total number of SCs in each field. Three independent experiments with two coverslips each were performed. Colocalization between 9-*O*-acetyl GD3 and *M. leprae*, laminin-2, β-dystroglycan, ErbB-2, and ErbB-3 receptors in both *in vivo* and *in vitro* assays was assessed with the colocalization graph function of the confocal software (Axiovision; Zeiss).

For quantification of the 9-*O*-acetyl GD3 immunoblockage assay, two independent experiments were performed on a total of eight wells for each experimental condition. Five photomicrographs were taken per coverslip, and the percentage of SCs with associated *M. leprae* was calculated for each experimental group. The number of bacteria per SC was also counted, and criteria were defined as low charge (1–5 bacteria/SC), medium charge (6–10 bacteria/SC), and high charge (11–15 bacteria/SC).

RESULTS

Expression of 9-O-Acetyl GD3 Ganglioside by Schwann Cells Associated with M. leprae—The first objective of this study was to determine whether the interaction between *M. leprae* (*M. leprae*-FITC$^+$, MOI = 1:10, 24 h of incubation) and Schwann
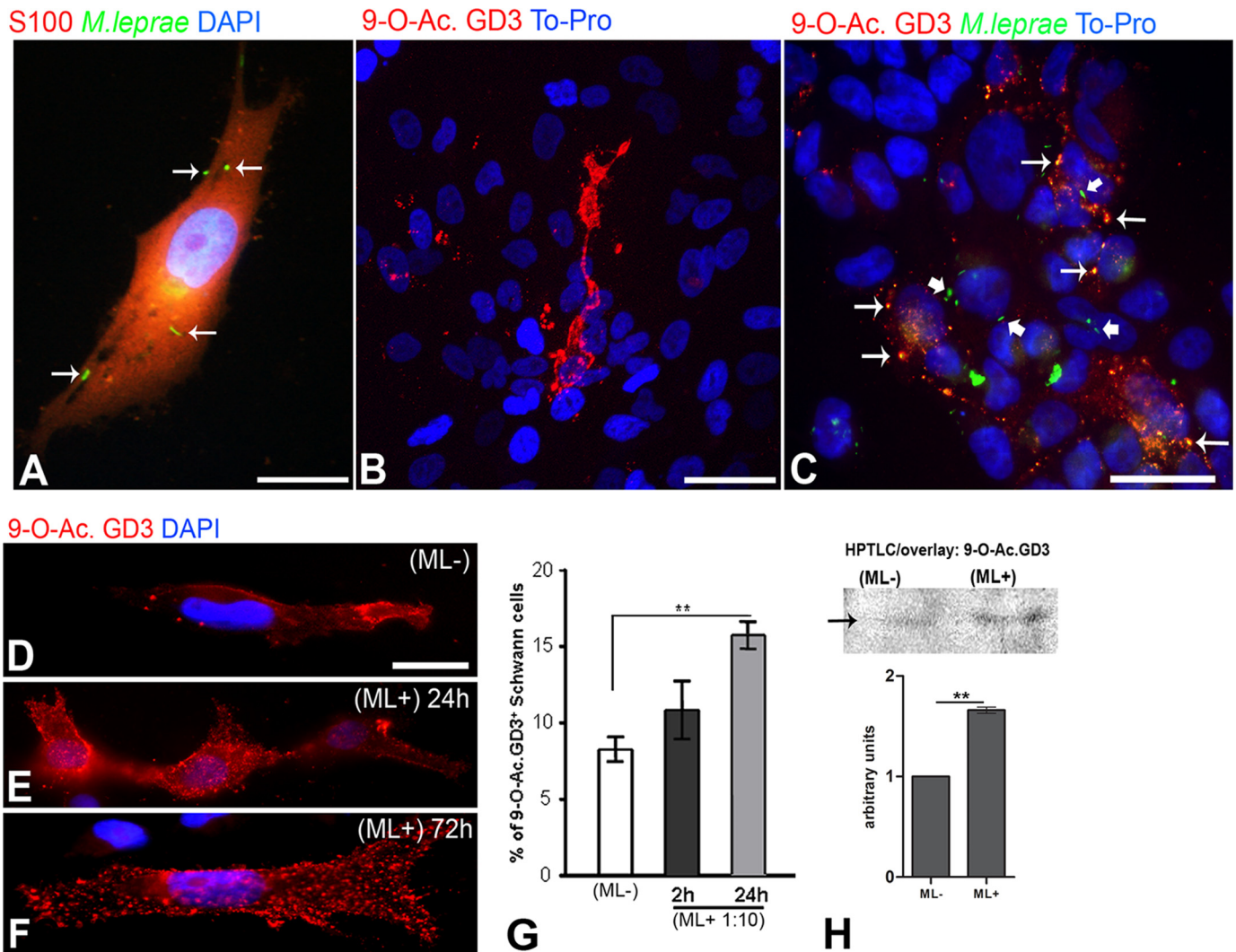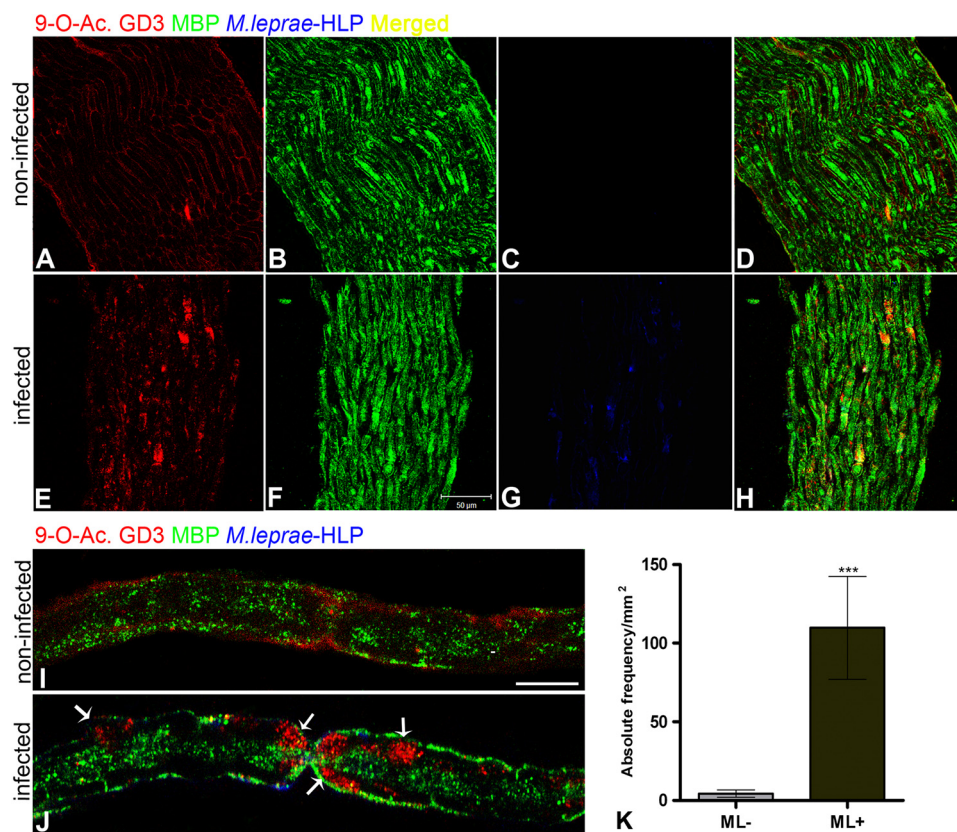
FIGURE 1. ***M. leprae* modulates 9-*O*-acetyl GD3 expression in Schwann cells.** *A*, epifluorescence image of SCs at low confluence incubated with FITC-labeled *M. leprae* (*green*) for 24 h and immunolabeled using IgG-Cy3 anti-S100 (*red*). The nuclei were counterstained with DAPI for epifluorescence imaging (*blue*). *B*, optical section of SCs incubated for 24 h without ML and immunolabeled using anti-9-*O*-acetyl GD3 IgM (*red*). The nuclei were counterstained with To-Pro for confocal imaging (*blue*). *C*, optical section of SCs incubated with FITC-labeled *M. leprae* for 24 h and immunolabeled for 9-*O*-acetyl GD3. Points of colocal-ization can be observed in *yellow* (*thin arrows*), and non-colocalized bacteria are indicated by *thick arrows*. *D–F*, high magnification epifluorescence images of SCs immunolabeled for 9-*O*-acetyl GD3 (*red*): noninfected (*D*) and incubated with ML for 24 h (*E*) or 72 h (*F*). *G*, percentage of cultured SCs expressing 9-*O*-acetyl GD3 after incubation for 2 or 24 h with ML (*ML+*, multiplicity of infection: 1:10) or in the absence of ML (*ML-*). *H*, HPTLC followed by overlay and immunoblotting, showing increasing amounts of 9-*O*-acetyl GD3 in SCs incubated with or without ML. *, $p < 0.01$; *, $p < 0.001$ (ANOVA). $n = 8$ samples for each experimental condition. *Scale bars*, *A*, *B*, and *D–F*, 20 μm; *C*, 50 μm.

cells (immunostained for S100) was able to modify 9-*O*-acetyl GD3 abundance or distribution, as observed by epifluorescent microscopy. Fig. 1*A* shows internalized and surface-associated bacteria in SCs. Expression of 9-*O*-acetyl GD3 ganglioside was detected by compression of several optical sections of the same area obtained by laser scanning microscopy (Fig. 1*B*, bi-dimensional reconstruction). Not all SCs expressed the ganglioside, but a higher number of ganglioside-positive cells were visible when inactivated ML was added to the culture (Fig. 1*C*). Different patterns of 9-*O*-acetyl GD3 expression were observed in each of the two conditions, from large membrane clusters along the surface on noninfected cells (Fig. 1*B*) to a punctate membrane signal similar to lipid rafts in bacillus-exposed cells (Fig. 1*C*). Many points of colocalization of 9-*O*-acetyl GD3 and ML were visible on SC surfaces (Fig. 1*C*, *thin arrows*). However, there were also non-colocalized bacteria and gangliosides pres-

ent on the SC surfaces (Fig. 1*C*, *thick arrows*). The distribution of 9-*O*-acetyl GD3 on SCs was observed in a time course of incubation with ML (2, 12, 24, 48, and 72 h) and compared with the control group, where ML was not added (Fig. 1, *D–F*). The control cells displayed weak and homogeneous expression of 9-*O*-acetyl GD3 (Fig. 1*D*). This differed markedly from the increased and punctuated expression of the ganglioside along SC surfaces from early to late incubation times, which can be clearly seen in Fig. 1 (*E* and *F*). Quantitative analysis of the number of 9-*O*-acetyl GD3-positive SCs was performed after 24 h of exposure to ML (Fig. 1*G*, MOI = 10:1) and showed a statistically significant increase, from 8.1 $\pm$ 0.2 to 15.2 $\pm$ 0.3%. Biochemical analysis by HPTLC of samples from SC cultures in the presence or absence of ML confirmed the increase in 9-*O*-acetyl GD3 synthesis in the experimental group compared with control (Fig. 1*H*).

FIGURE 2. ***M. leprae*** **modulates 9-*O*-acetyl GD3 expression and distribution in the sciatic nerve *in vivo*.** Optical longitudinal sections by confocal microscopy of noninfected (*A–D*) and infected (*E–H*) sciatic nerve, triple-immunostained for 9-*O*-acetyl GD3 (*A* and *E*), MBP (*B* and *F*), and ML HLP (*C* and *G*). Merged images are shown in *D* and *H*. *I* and *J*, confocal optical slices at high magnification of noninfected (*I*) or ML-infected (*J*) isolated sciatic-nerve fibers triple immunostained for 9-*O*-acetyl GD3, MBP, and HLP. The *arrows* in *J* indicate clusters of the ganglioside at the Ranvier's node area and along the infected nerve fiber. *n* = 4 mice for each experimental condition. *K*, histogram of quantitative analysis by confocal microscopy of the expression of 9-*O*-acetyl GD3 ganglioside in longitudinal sections of infected (*ML*+) or noninfected (*ML*-) sciatic nerve of NUDE mice. ***, *p* < 0.0001 (Mann-Whitney). *Scale bars*, *A–H*, 50 μm; *I* and *J*, 200 μm.

nerves infected with ML (Fig. 2*H*, *yellow*). As seen *in vitro*, ganglioside distribution changed from diffuse (noninfected) to clustered patterns along the infected nerve fiber (Fig. 2, *A*, *E*, *I*, and *J*). The Ranvier's node area is shown in high magnification confocal images (Fig. 2, *I* and *J*, *arrows*). HLP staining in blue can be observed at the Ranvier's node, as well as at some points along the nerve fiber (Fig. 2*J*). Is important to notice that the HLP antigen immunolocalization signal did not necessarily represent an intact and viable bacillus; it seems that the tissue came from an animal after 10 months of chronic infection. Fluorescence analysis by confocal microscopy showed significant up-regulation of 9-*O*-acetyl GD3 in infected NUDE mice (Fig. 2*K*). Taken together, these data suggest that ML infection leads to increased amounts of 9-*O*-acetyl GD3 and changes its cell membrane distribution along the nerve fiber. Furthermore, these changes are probably associated with the presence of the pathogen or pathogen-derived antigens. Immunostaining of another ML antigen (LAM) in the same infected tissue also showed points of colocalization between ML and 9-*O*-acetyl GD3 ganglioside (supplemental Fig. S2*D, arrows*).

9-O-Acetyl GD3 Ganglioside Associated with β-Dystroglycan and ErbB-2 Receptors in Schwann Cells Exposed to M. leprae— Because we observed a high degree of colocalization between ML and 9-*O*-acetyl GD3 during *in vitro* SC infection (Fig. 1), we next investigated whether the membrane pool of ganglioside was associated with molecules known to be related to ML attachment and invasion following ML exposure. SCs were incubated with ML for 24 h, and coimmunoprecipitation and colocalization experiments were performed to monitor the association between 9-*O*-acetyl GD3 and laminin-2, β-dystroglycan, or ErbB-2 receptors.

Following ganglioside immunoprecipitation from SCs incubated with or without ML for 24 h, Western blots were performed for each ML ligand (Fig. 3*A*). Levels of the α-chain of laminin-2 (300 kDa) were not significantly different between untreated and bacteria-exposed SCs. However, quantitative analysis of the immunoblots against β-dystroglycan and ErbB-2 receptor showed 3- and 5-fold higher levels, respectively, in ML-treated SCs compared with the control group. β-Dystroglycan was not coimmunoprecipitated using anti-A2B5 antibody or isotype mouse IgM, but a visible β-dystroglycan signal was obtained by immunoprecipitating with anti-laminin-2 (Fig. 3*B*).

SCs were also incubated with other mycobacteria (*M. bovis* BCG, pathogenic; and *M. smegmatis*, nonpathogenic) for 24 h (supplemental Fig. S1, *C–F*). Quantitative analysis showed that both *M. smegmatis* and *M. bovis* BCG displayed less association with SCs (supplemental Fig. S1*G*; ANOVA *p* < 0.01) and less association with 9-*O*-acetyl GD3 ganglioside than did ML (supplemental Fig. S1*H*; ANOVA *p* < 0.01).
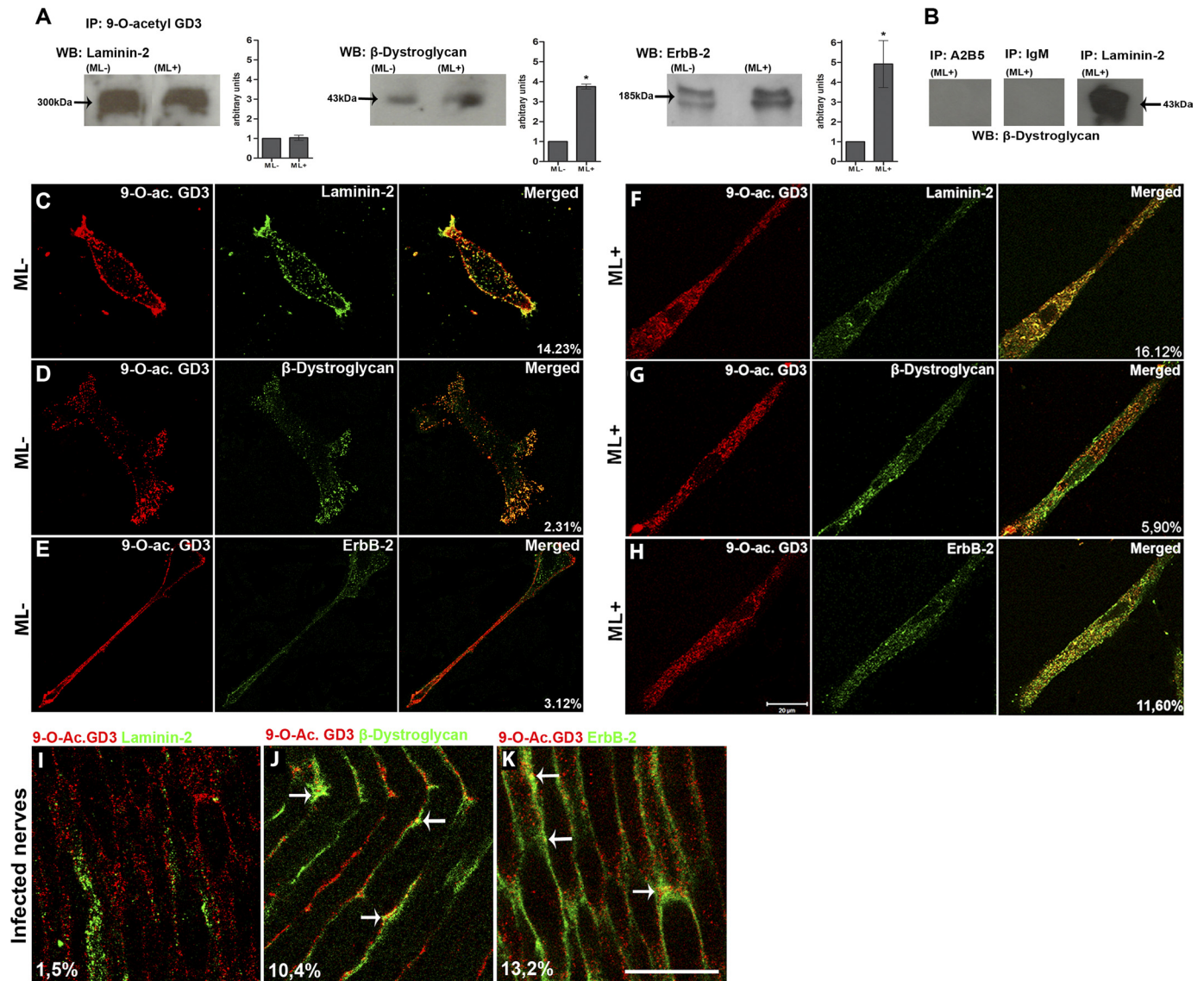
*Expression of 9-O-Acetyl GD3 Ganglioside in Nerve Fibers Is Positively Affected by M. leprae Infection—*The second aim of this study was to determine whether the SC ganglioside modulation observed *in vitro* is biologically relevant *in vivo*. To address this point, Balb-C Fox^nu/nu (NUDE mice) mice were infected with ML in the booth posterior foot pad, as described by Colston and Hilson in 1976 (26). Ten months after infection, the animals were sacrificed, and the sciatic nerves were isolated and processed for histological analysis. Optical longitudinal sections of the sciatic nerves of NUDE mice triple-immunostained for 9-*O*-acetyl GD3, MBP, and HLP (ML antigen marker) showed increased expression and redistribution of 9-*O*-acetyl GD3 in nerves isolated from mice infected with ML compared with the control group (Fig. 2, *A* and *E*). We did not observe changes in MBP levels in infected mice, even at 10 months after infection (Fig. 2, *B* and *F*). On the other hand, 9-*O*-acetyl GD3-MBP colocalization seems to increase in

FIGURE 3. **9-O-Acetyl GD3 ganglioside associates with laminin-2, β-dystroglycan, and ErbB-2 receptor on the Schwann cell surface *in vitro* and *in vivo*.** *A*, coimmunoprecipitation (*IP*) of 9-O-acetyl GD3 with laminin-2, β-dystroglycan, and ErbB-2 receptor in the absence (*ML-*) or presence (*ML*+) of *M. leprae* with histograms of quantitative analysis by densitometry for each protein analyzed by Western blotting (*WB*). *B*, as coimmunoprecipitation controls, anti-A2B5, mouse IgM isotype, and anti-laminin-2 were used, followed by Western blotting for β-dystroglycan. Control groups (*ML-, n* = 3) were normalized to 1 for comparison (*ML*+, *n* = 3). *C–H*, confocal sections of semi-confluent Schwann cells, uninfected (*C–E*) or after 48 h of ML exposure (*F–H*), double-immunolabeled for 9-O-acetyl GD3 and laminin-2 (*C* and *F*), β-dystroglycan (*D* and *G*), and ErbB-2 receptor (*E* and *H*). *Right-hand columns* (*C–E* and *F–H*) show merged images, where *yellow dots* represent colocalization. The percentages in *C–E* and *F–H* represent the degree of colocalization of 9-O-acetyl GD3 with laminin-2, β-dystroglycan, or ErbB-2 receptor in the presence or absence of ML. *I–K*, confocal longitudinal optical sections of NUDE mice sciatic nerves infected by *M. leprae* double-labeled for 9-O-acetyl GD3 and laminin-2, β-dystroglycan, or ErbB-2 receptor. Points of colocalization are indicated by *arrows*. The percentages in *I–K* represent the degree of colocalization. *, *p* < 0.01 (Mann-Whitney). *n* = 3 experiments for each ML ligand analyzed. *Scale bars, C–K,* 20 μm.

We also investigated the colocalization of 9-*O*-acetyl GD3 and ML receptor association by laser confocal microscopy. Semi-confluent cultures were double-labeled for 9-*O*-acetyl GD3 and laminin-2, β-dystroglycan, or ErbB-2 receptor, and colocalization ratios were measured. Quantitative analysis gave colocalization values 14.2% for laminin-2 (Fig. 3*C*), 2.3% for dystroglycan (Fig. 3*D*) and 3.12% for ErbB-2 (Fig. 3*E*) in untreated cells. Colocalization ratios increased dramatically in ML-exposed cultures to 16.12% for laminin-2 (Fig. 3*F*), 5.9% for dystroglycan (Fig. 3*G*), and 11.6% for ErbB-2 (Fig. 3*H*). The most significant increases in colocalization with 9-*O*-acetyl GD3 were observed for dystroglycan (Fig. 3*B*) and ErbB-2 (Fig. 3*C*), whereas colocalization with laminin-2 was not signifi-

cantly affected (Fig. 3*A*). Yellow points on the SC surface (Fig. 3, *F–H, right column*) show the colocalization between 9-*O*-acetyl GD3 and the previously described ML receptors. As a colocalization control, SC cultures were also double-labeled for laminin-2 (ligand) and β1-integrin (receptor subunit) in the presence or absence of ML. β1-Integrin is not involved in ML-SC adhesion, and we observed no differences in the pattern of expression of β1-integrin or colocalization with laminin-2 in either experimental condition (supplemental Fig. 3, *A–F*).

In vivo analyses of 9-*O*-acetyl GD3 colocalization with the three ML receptors were performed to confirm the *in vitro* findings. Longitudinal frozen sections of infected sciatic nerves of NUDE mice were double-labeled for 9-*O*-acetyl GD3 gangli-
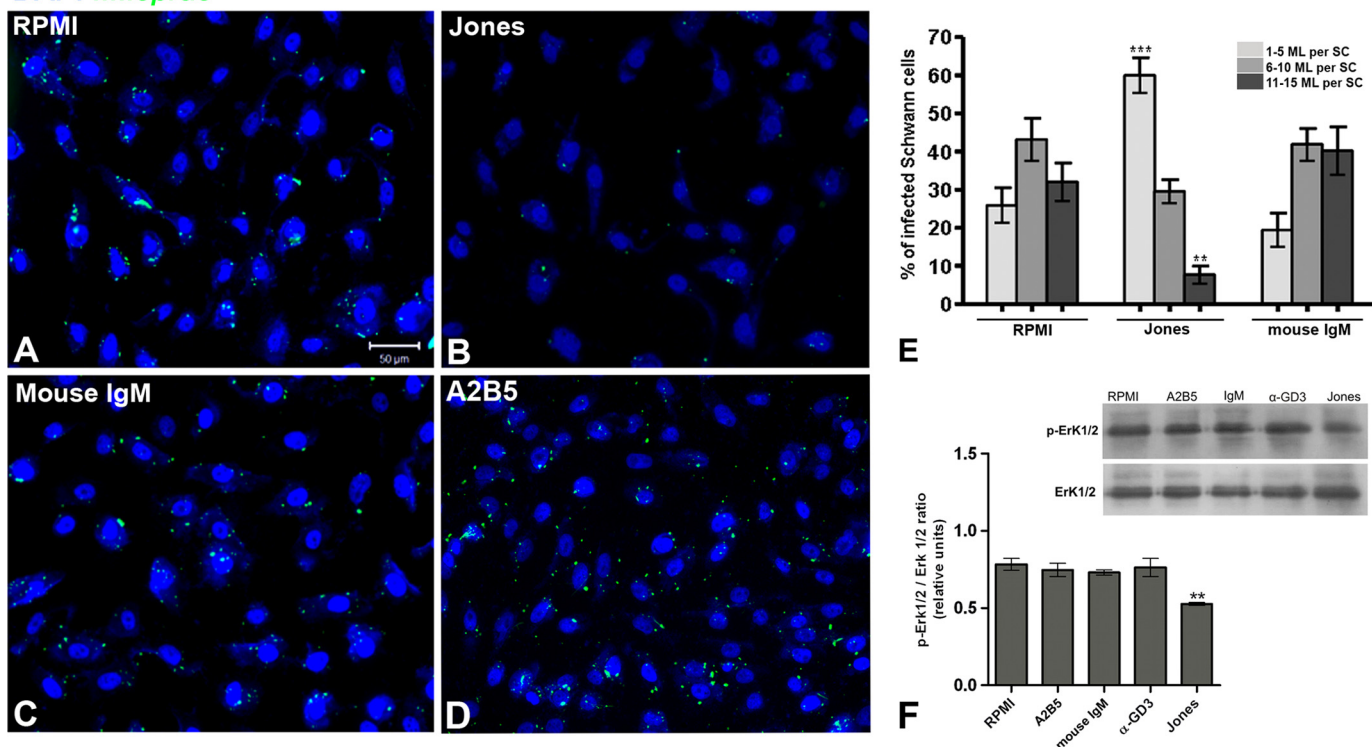
FIGURE 4. **Immunoblockage of 9-*O*-acetyl GD3 reduces the association of *M. leprae* with Schwann cells *in vitro*.** *A–D*, epifluorescence images of SC nuclei (DAPI) incubated for 24 h with FITC-labeled *M. leprae* or RPMI alone control medium (*A*), Jones (mAb α-9-*O*-acetyl GD3) antibody added to the control medium (*B*), mouse IgM isotype added to the control medium (*C*) or A2B5 antibody added to the control medium (*D*). *E*, percentage of SCs associated with ML with different numbers of bacteria/cell (1–5, 6–10, and 11–15 bacteria/cell). *F*, Western blotting and quantitative analysis of the active ERK 1/2 (p-ERK 1/2) from SCs cultured for 48 h with ML or incubated with RPMI (standard medium), A2B5 mAb, and Jones mAb. Western blotting for active ERK 1/2 (p-ERK 1/2) and total ERK 1/2 following the same experimental conditions. ***, $p < 0.0001$; **, $p < 0.001$ (ANOVA). Two independent experiments were performed for each experimental condition ($n = 8$). *Scale bars*, *A–C*, 50 μm.

oside and laminin-2, β-dystroglycan, or ErbB-2. Optical sections obtained by laser scanning microscopy allowed us to observe areas of colocalization (Fig. 3, *I–K*). These assays demonstrated colocalization between the ganglioside and β-dystroglycan or ErbB-2 receptor in NUDE infected nerves but not between the ganglioside and laminin-2 (Fig. 3, *I–K, arrows*). Taken together, the colocalization and coimmunoprecipitation suggest that ML adhesion to the SC surface induces the association of 9-*O*-acetyl GD3 ganglioside with β-dystroglycan and ErbB-2.

Neutralization of 9-O-Acetyl GD3 Reduces Association of M. leprae to Schwann Cells—We have shown the association between ML and 9-*O*-acetyl GD3 ganglioside on the membranes of SCs prior to invasion (Fig. 1) and demonstrated that this association induces 9-*O*-acetyl GD3 association with molecules already known to participate in ML adhesion and infection in SCs (Fig. 3). We next asked whether we could block ML invasion using anti-9-*O*-acetyl GD3 antibody *in vitro*. Indeed, the neutralization of 9-*O*-acetyl GD3 by its monoclonal antibody (Jones clone; Fig. 4*B*) dramatically reduced ML adhesion to SCs (Fig. 4*A*), leading to a reduction in the percentage of SCs with high numbers of ML (11–15 bacilli/cell; Fig. 4*E*) and an increase in the percentage of SCs with low numbers of ML (1–5 bacilli/cell; Fig. 4*E*). Mouse IgM immunoglobulin, a control for immunoglobulin isotype, did not induce any significant change in ML association (Fig. 4*C*). The addition of anti-A2B5 also failed to reduce ML association with SCs (Fig. 4*D*). The levels of

laminin-2, β-dystroglycan, and ErbB-2 on SC surfaces 24 h after incubation with the neutralizing Jones mAb (supplemental Fig. S4) did not change, which rules out the possibility of antibody-induced down-regulation of the receptors.

Previous work described that Jones antibody could also recognize integrins (25). To ensure that the immunoblockage of ML internalization by Jones is a specific effect exerted by 9-*O*-acetyl GD3 and not by integrin blockage, we performed a control using β1-integrin blocking peptide. After 2 h of incubation with 100 ng/ml of β1-integrin blocking peptide followed by 24 h of incubation with mAb Jones, we observed significantly reduced percentage of Schwann cells associated with ML compared with the control condition with the blocking peptide alone and RPMI medium (supplemental Fig. S5). The minor reduction of ML-Schwann cell association observed when cells were preincubated with β1-integrin blocking peptide is probably due to the role of β1-integrin as a laminin-binding protein, because laminin is recognized by ML and exerts a crucial contribution to cellular invasion (27).

We also performed another approach to neutralize 9-*O*-acetyl GD3 ganglioside incubating live cultured Schwann cells with 10 mM $NaIO_4$ for 1 h at 4 °C in the absence of light. It is well known that periodate (IO_4^-) breaks the bond between carbons 7 and 8 of the sialic acid moiety of 9-*O*-acetyl GD3 (Fig. 5, *A* and *B*) (23, 24). We did not observe any signal of 9-*O*-acetyl GD3 in Schwann cells treated with 10 mM periodate (Fig. 5*E*), when compared with untreated cells (Fig. 5*F*). Treatment of Schwann
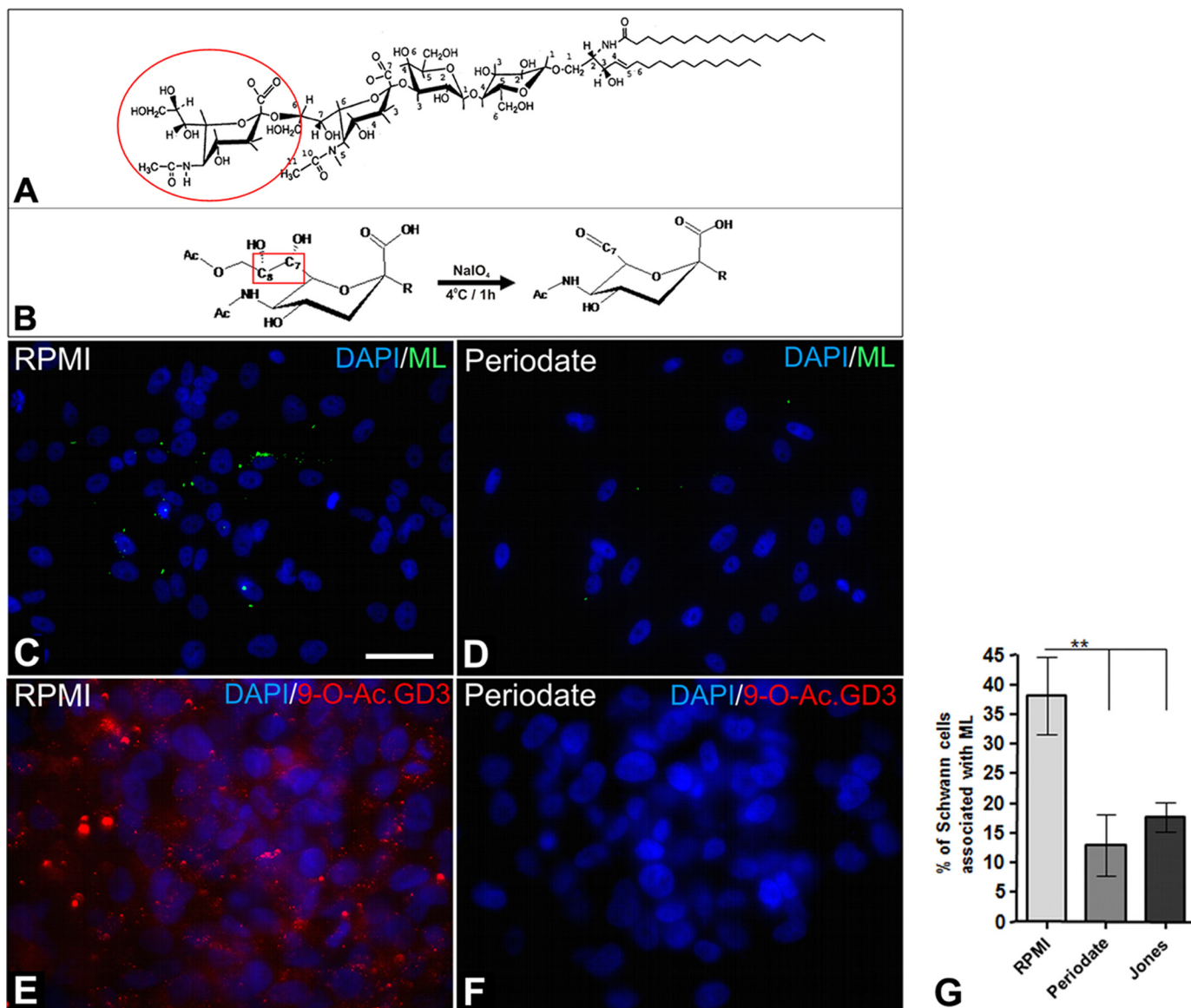
FIGURE 5. **Deacetylation of 9-*O*-acetyl GD3 reduces the association of *M. leprae* with Schwann cells *in vitro*.** *A*, molecular structure of 9-*O*-acetyl GD3 ganglioside. The second sialic acid is demonstrated by a *red circle*. *B*, suggested mechanism for the removal of *O*-acetyl group by breaking the bond between carbons number seven and eight of the second sialic acid. *C* and *D*, epifluorescence images of cultured Schwann cells 24 h after exposition to FITC-labeled *M. leprae* treated (*D*) or not (*C*) with sodium periodate (NaIO$_4$) for 1 h at 4 °C in the absence of light. The cell nuclei were counterstained with DAPI. *E* and *F*, immunofluorescence for 9-*O*-acetyl GD3 ganglioside (*E*) was also performed after deacetylation of the ganglioside by NaIO$_4$ (*F*). All of the experimental conditions were performed for 1 h at 4 °C in the absence of light. *G*, quantitative analysis of the percentage of Schwann cells associated with ML (24 h of exposition) after incubation with RPMI medium, NaIO$_4$, or Jones (mAb α-9-*O*-acetyl GD3) neutralizing antibody. **, $p < 0,001$ ANOVA. Two independent experiments were performed for each experimental condition ($n = 4$). *Ac*, acetyl group; *R* = radical. *Scale bars*, *C* and *D*, 50 μm; *E* and *F*, 20 μm.

cell with 10 mM periodate significantly reduced the number of cells associated with ML (Fig. 5, *C*, *D*, and *G*).

M. leprae-induced ERK 1/2 Activation and Schwann Cell Proliferation Is Abolished by Immunoblockage of 9-O-Acetyl GD3 Ganglioside—ERK 1/2 activation by internalized ML, which leads to demyelination of SCs, is also associated with SC proliferation (6). Because ERK 1/2 activation is a part of the MAPK pathway, and both proliferation and demyelination are activated by intracellular ML (8), we investigated whether cell proliferation induced by ML through ERK 1/2 could be reversed by 9-*O*-acetyl GD3 ganglioside immunoblockage. ERK 1/2 phosphorylation was measured by Western blotting in SC cultures exposed to inactivated ML (Fig. 4*E*). Quantitative anal-

ysis showed that activation of ERK 1/2 was reduced to low levels when 9-*O*-acetyl GD3 was preincubated with blocking antibody (Fig. 4*E*). A2B5, mouse IgM, or anti-GD3 treatment did not reduce phosphorylation of ERK 1/2 (Fig. 4*E*). Incubation with ML for 48 h increased the number of Ki-67-positive SCs by 19% (Fig. 6, *A*, *B*, and *E*, $p < 0.01$ ANOVA). Conversely, the number of Ki-67-positive cells in ML-exposed cultures in which 9-*O*-acetyl GD3 was neutralized was reduced by 21% (Fig. 6, *B*, *C*, and *E*, $p < 0.001$ ANOVA). Jones antibody alone, in the absence of ML, did not significantly reduce cell proliferation compared with the control group (Fig. 6*E*). We also tested immunoblockage on infected cells using mouse IgM, A2B5, and α-GD3 neutralizing antibodies. The percentages of Ki-67-pos-
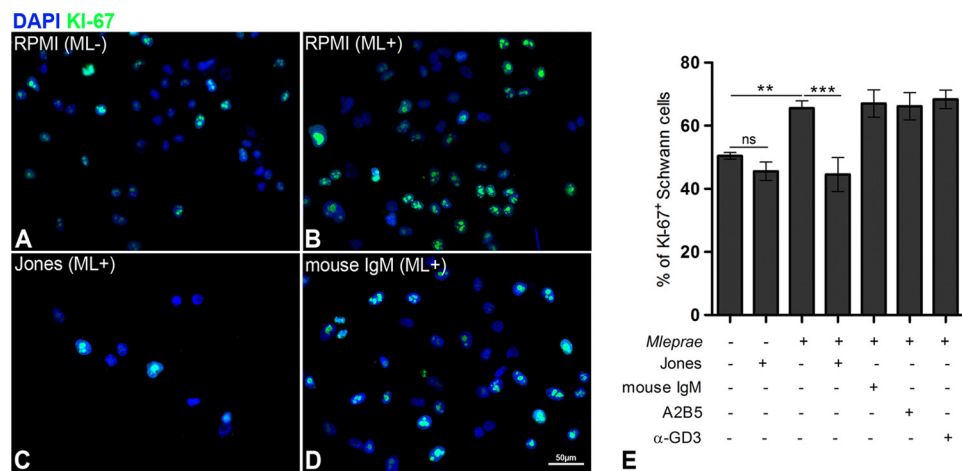
FIGURE 6. **Immunoblockage of 9-O-acetyl GD3 reduces Schwann cell proliferation induced by *M. leprae* in vitro.** *A–D*, epifluorescence images of SCs incubated for 48 h with RPMI alone (*A*), RPMI plus ML (*B*), Jones mAb plus ML (*C*), and mouse IgM plus ML (as isotype control for Jones mAb) (*D*). Fixed cultures were immunolabeled for Ki-67 and counterstained with DAPI. *E*, percentage of Ki-67$^+$ cells plus Jones mAb in the presence of absence of ML or with anti-A2B5 or anti-α-GD3 antibodies in the presence of ML as controls. *, < 0.01; **, $p < 0.001$ (ANOVA). Two independent experiments were performed for each experimental condition (*n* = 8). *Scale bars*, *A–D*, 50 μm.

itive SCs were similar to controls in each of these antibody-treated groups (Fig. 6*E*). In conclusion, immunoblockage of 9-O-acetyl GD3 was sufficient to inhibit SCs proliferation and ERK 1/2 activation induced by ML association.

DISCUSSION

In this study, we showed that ML induced increases in the cell surface expression and changes in the distribution of the 9-O-acetyl GD3 ganglioside in SC membranes *in vitro* as well as in the infected peripheral nerves of NUDE mice *in vivo*. The total amount of this ganglioside was increased by 70% (Fig. 1*H*) in the cultures incubated with ML (Fig. 1*C*). Changes in the expression of this ganglioside in Ml-infected nerves, especially concentrated at Ranvier's node, support the hypothesis that the 9-O-acetyl GD3 pool is somehow modified during ML infection in the nerves (Fig. 2*J*). Because increased ganglioside synthesis has been observed in ML-infected armadillos, this is likely an evolutionarily conserved response to the infection (28). Thus, we propose that ML evolved antigens able to generate these changes in ganglioside presentation, which will help and support bacillus infection of human nerves.

It is generally accepted that aggregated ML derived from lymphatic and blood vessels reach and bind to the endoneurial compartment of nerves through the circulatory system (29–31). Furthermore, ML can infect the dermis and directly bind to dermal SCs, where it can migrate along nerve fibers toward the dorsal roots (32). In both strategies of nerve infection, the internodal area seems to be a trophic niche for ML. These experiments showed that 9-O-acetyl GD3 is much more abundant in infected nerves (Fig. 1) and is concentrated on the internodal area (Fig. 2, *I–J*), which may facilitate subsequent ML attachment and invasion, because 9-O-acetyl GD3 immunoblockage dramatically reduced ML attachment (Fig. 4). A high amount of 9-O-acetyl GD3 on the SC membrane of infected nerves could induce cell proliferation signal transduction through the ERK 1/2 pathway (Figs. 4*E* and 6), leading to an increase in the num-

ber of unmyelinated cells, the primary cell target of the bacillus (8), with a resulting loss of myelination.

Other mycobacterium species with a similar hydrophobic envelop, such as *M. smegmatis*, *Mycobacterium tuberculosis*, and *Mycobacterium chelonae*, are able to bind laminin-2 and interact with SCs as well, suggesting a conserved feature within the genus *Mycobacterium* (33). However, the association of 9-O-acetyl GD3 on the SC membrane with other *Mycobacterium* species (*M. bovis* and *M. smegmatis*) is significantly reduced compared with ML (supplemental Fig. S1*H*), suggesting a specific adaptation of ML surface antigens to bind to the ganglioside, rather than a simple hydrophobic interaction.

The neutralization or deacetylation of 9-O-acetyl GD3 ganglioside with Jones mAb or meta sodium periodate significantly reduced the association of ML to SCs and effectively reduced levels of infection (bacilli/cell) (Figs. 4 and 5). Only a small fraction of the cells presented high infection rates (11–15 bacilli/cell) in control groups (Fig. 4) and that population was reduced by two-thirds with 9-O-acetyl GD3 immunoblockage. It is possible that the heterogeneity of ML infection *in vitro* is due to the fact that only a small fraction of the cells endogenously express the 9-O-acetyl GD3 ganglioside (Fig. 1).

Internalized ML is known to trigger the alternative MAPK signaling pathway (PKC$_\xi$-LcK-ERK 1/2) (8); therefore, the reduced activation of ERK 1/2 in the presence of Jones mAb probably reflects the reduced amount of ML inside the SCs. The addition of anti-A2B5 antibody, which neutralizes gangliosides of the C-path synthesis, did not have the same effect (data not shown). Finally, neutralizing 9-O-acetyl GD3 ganglioside abolished the proliferation induced by ML in SCs (Fig. 6). In this study, we examined SC proliferation after immunoblockage of 9-O-acetyl GD3 48 h after incubating with ML. Whereas this may be too short a time to measure proliferation assay in normal SCs, the ST-8814 Schwannoma cell line has an increased proliferation rate compared with primary SC cultures (19). Thus, this cell type allowed us to analyze SC proliferation in the absence of ganglioside in a relatively short time period.

Gangliosides are smaller in size than most cell surface proteins or glycoproteins. The extracellular tail of 9-O-acetyl GD3 comprised of four carbohydrates aligned toward the extracellular matrix (9). This reduces the possibility that this molecule acts as a direct receptor for ML, but it supports the hypothesis that this ganglioside is an important coreceptor to ML. Additionally, several published reports indicate that deacetylated or neutralized 9-O-acetyl GD3 ganglioside has important roles in neural and immune cell processes, such as cell adhesion, migration, and survival (13, 34). Neutrophil motility is sharply reduced when GM1 gangliosides are neutralized (35). Migrat-

ing neurons in the developing cerebral cortex, subventricular zone, or cerebellum are also affected after immunoblockage of 9-*O*-acetyl GD3 ganglioside (11, 13, 14). Gangliosides are known to interact laterally in the membrane, regulating the responsiveness of receptors for insulin, epidermal growth factor, and vascular endothelial growth factor (36). Gangliosides also act as regulatory elements in the immune and nervous systems, in metabolism, during cancer progression, and in apoptosis inhibition (10, 36–39). The ganglioside 9-*O*-acetyl GD3 could thus be involved in regulating the extracellular localization of membrane proteins recognized by ML such as β-dystroglycan and ErbB-2. Because 9-*O*-acetyl GD3 has been reported to be present in lipid rafts (40), we hypothesize that the punctate distribution of this ganglioside induced by the bacillus could be an effect of its sequestration to lipid rafts (Fig. 2*J*).

Studies by Rambukkana and co-workers (3, 6) demonstrated the involvement of molecules such as dystroglycan, laminin-α2, and ErbB-2 receptor as key players for SC infection by ML. In the present work we demonstrated the association of 9-*O*-acetyl GD3 with two of three molecules described above, β-dystroglycan and ErbB-2, after ML exposure (Fig. 3). Laminin-2 is not attached directly to the cell surface of SCs, as opposed to β-dystroglycan or ErbB-2 receptor but can be found in a soluble form in the extracellular matrix or bound to the extracellular matrix or cell membrane (41). We did not observe points of colocalization of laminin-2 and 9-*O*-acetyl GD3 in the infected nerve tissue, whereas such points were clearly seen for β-dystroglycan and ErbB-2 at high magnifications with confocal microscopy (Fig. 3, *I–K*). This suggests that, unlike the other ligands for ML, laminin-2 is not in contact with 9-*O*-acetyl GD3. In addition, increased levels of ErbB-2 were found after immunoprecipitation of 9-*O*-acetyl GD3 in SCs incubated with ML, which suggests a universal involvement of this ganglioside during infection of myelinated and nonmyelinated SCs. The colocalization of ErbB-2 and 9-*O*-acetyl GD3 in infected nerves supports this hypothesis because ErbB-2 is the ML receptor in myelinated SCs (Fig. 3, *A*, *E*, and *K*). Interestingly, dystroglycan, which is highly expressed at the nodal area in the nodes of Ranvier, is essential for regular myelination and establishment of nodal architecture (42). Among its biological roles is clustering of voltage-gated sodium channels at nodes of Ranvier in SCs (43). We observed ML antigen as well as colocalization of dystroglycan and 9-*O*-acetyl GD3 in the same area at these nodes (Fig. 3*J*). Therefore, it is possible that ML disrupts dystroglycan function at nodal areas, causing a loss of function of myelinating fibers through an unknown molecular process.

In conclusion, the data presented here suggest a biological role for 9-*O*-acetyl GD3 in the infection of Schwann cells with *M. leprae*. This is the first report on the important role of a host cell ganglioside in mycobacterium infection. Our study sheds light on the adhesion of ML to SCs, an event that depends on a combination of several elements on the SC membrane. Further studies are necessary to clarify whether other SC membrane elements can interact with 9-*O*-acetyl GD3 and to determine the impact of these associations on nerve demyelination during leprosy.

REFERENCES

1. Scollard, D. M., Adams, L. B., Gillis, T. P., Krahenbuhl, J. L., Truman, R. W., and Williams, D. L. (2006) *Clin. Microbiol. Rev.* **19,** 338–381
2. Rambukkana, A. (2000) *Lepr. Rev.* **71,** (suppl.) S168–S169
3. Rambukkana, A., Yamada, H., Zanazzi, G., Mathus, T., Salzer, J. L., Yurchenco, P. D., Campbell, K. P., and Fischetti, V. A. (1998) *Science* **282,** 2076–2079
4. Ng, V., Zanazzi, G., Timpl, R., Talts, J. F., Salzer, J. L., Brennan, P. J., and Rambukkana, A. (2000) *Cell* **103,** 511–524
5. Rambukkana, A., Zanazzi, G., Tapinos, N., and Salzer, J. L. (2002) *Science* **296,** 927–931
6. Tapinos, N., Ohnishi, M., and Rambukkana, A. (2006) *Nat. Med.* **12,** 961–966
7. Jessen, K. R., and Mirsky, R. (2008) *Glia* **14,** 1552–1565
8. Tapinos, N., and Rambukkana, A. (2005) *Proc. Natl. Acad. Sci. U.S.A.* **102,** 9188–9193
9. Thompson, T. E., and Tillack, T. W. (1985) *Annu. Rev. Biophys. Biophys. Chem.* **14,** 361–386
10. Kniep, B., Kniep, E., Ozkucur, N., Barz, S., Bachmann, M., Malisan, F., Testi, R., and Rieber, E. P. (2006) *Int. J. Cancer* **119,** 67–73
11. Mendez-Otero, R., and Cavalcante, L. A. (2003) *Prog. Mol. Subcell Biol.* **32,** 97–124
12. Mendez-Otero, R., and Santiago, M. F. (2003) *Braz. J. Med. Biol. Res.* **36,** 1003–1013
13. Santiago, M. F., Costa, M. R., and Mendez-Otero, R. (2004) *J. Neurosci.* **24,** 474–478
14. Miyakoshi, L. M., Mendez-Otero, R., and Hedin-Pereira, C. (2001) *Braz. J. Med. Biol. Res.* **34,** 669–673
15. Mendez-Otero, R., and Friedman, J. E. (1996) *Eur. J. Cell Biol.* **71,** 192–198
16. Malisan, F., and Testi, R. (2002) *Biochim. Biophys. Acta* **1585,** 179–187
17. Schlosshauer, B., Blum, A. S., Mendez-Otero, R., Barnstable, C. J., and Constantine-Paton, M. (1988) *J. Neurosci.* **8,** 580–592
18. Ribeiro-Resende, V. T., Oliveira-Silva, A., Ouverney-Brandão, S., Santiago, M. F., Hedin-Pereira, C., and Mendez-Otero, R. (2007) *Neuroscience* **147,** 97–105
19. Svaren, J., and Meijer, D. (2008) *Glia* **56,** 1541–1551
20. Rodrigues, L. S., da Silva Maeda, E., Moreira, M. E., Tempone, A. J., Lobato, L. S., Ribeiro-Resende, V. T., Alves, L., Rossle, S., Lopes, U. G., and Pessolani, M. C. (2010) *Cell Microbiol.* **12,** 42–54
21. Shepard, C. C., and McRae, D. H. (1968) *Int. J. Lepr. Other Mycobact. Dis.* **36,** 78–82
22. Santiago, M. F., Berredo-Pinho, M., Costa, M. R., Gandra, M., Cavalcante, L. A., and Mendez-Otero, R. (2001) *Mol. Cell Neurosci.* **17,** 488–499
23. Van Lenten, L., and Ashwell, G. (1971) *J. Biol. Chem.* **246,** 1889–1894
24. Manzi, A. E., Dell, A., Azadi, P., and Varki, A. (1990) *J. Biol. Chem.* **265,** 8094–8107
25. Yang, C. R., Liour, S. S., Dasgupta, S., and Yu, R. K. (2007) *J. Neurosci. Res.* **85,** 1381–1390
26. Colston, M. J., and Hilson, G. R. (1976) *Nature* **262,** 399–401
27. Rambukkana, A., Salzer, J. L., Yurchenco, P. D., and Tuomanen, E. I. (1997) *Cell* **88,** 811–821
28. Harris, E. B., Li, Y. T., and Li, S. C. (1986) *Int. J. Lepr. Other Mycobact. Dis.* **54,** 289–293

29. Khanolkar, V. R. (1964) *Indian J. Med. Res.* **52,** 139–150
30. Katoch, V. M. (1999) *Indian J. Lepr.* **71,** 45–59
31. Scollard, D. M., McCormick, G., and Allen, J. L. (1999) *Am. J. Pathol.* **154,** 1611–1620
32. Scollard, D. M. (2000) *Microbes Infect.* **2,** 1835–1843
33. Marques, M. A., Antônio, V. L., Sarno, E. N., Brennan, P. J., and Pessolani, M. C. (2001) *J. Med. Microbiol.* **50,** 23–28
34. Mukherjee, P., Faber, A. C., Shelton, L. M., Baek, R. C., Chiles, T. C., and Seyfried, T. N. (2008) *J. Lipid Res.* **49,** 929–938
35. Gong, Y., Tagawa, Y., Lunn, M. P., Laroy, W., Heffer-Lauc, M., Li, C. Y., Griffin, J. W., Schnaar, R. L., and Sheikh, K. A. (2002) *Brain* **125,** 2491–2506
36. Regina Todeschini, A., and Hakomori, S. I. (2008) *Biochim. Biophys. Acta* **1780,** 421–433
37. Vyas, A. A., Patel, H. V., Fromholt, S. E., Heffer-Lauc, M., Vyas, K. A., Dang, J., Schachner, M., and Schnaar, R. L. (2002) *Proc. Natl. Acad. Sci. U.S.A.* **99,** 8412–8417
38. Vyas, K. A., Patel, H. V., Vyas, A. A., and Schnaar, R. L. (2001) *Biol. Chem.* **382,** 241–250
39. Vyas, A. A., and Schnaar, R. L. (2001) *Biochimie* **83,** 677–682
40. Simons, M., Schwarz, K., Kriz, W., Miettinen, A., Reiser, J., Mundel, P., and Holthöfer, H. (2001) *Am. J. Pathol.* **159,** 1069–1077
41. Hall, H., Bozic, D., Michel, K., and Hubbell, J. A. (2003) *Mol. Cell. Neurosci.* **24,** 1062–1073
42. Saito, F., Moore, S. A., Barresi, R., Henry, M. D., Messing, A., Ross-Barta, S. E., Cohn, R. D., Williamson, R. A., Sluka, K. A., Sherman, D. L., Brophy, P. J., Schmelzer, J. D., Low, P. A., Wrabetz, L., Feltri, M. L., and Campbell, K. P. (2003) *Neuron* **38,** 747–758
43. Occhi, S., Zambroni, D., Del Carro, U., Amadio, S., Sirkowski, E. E., Scherer, S. S., Campbell, K. P., Moore, S. A., Chen, Z. L., Strickland, S., Di Muzio, A., Uncini, A., Wrabetz, L., and Feltri, M. L. (2005) *J. Neurosci.* **25,** 9418–9427